International Journal of Engineering & Technology, 7 (4.8) (2018) 7-16

International Journal of Engineering & Technology

Website: www.sciencepubco.com/index.php/IJET

Research paper

Decomposition of Hydrates under the Action of Ultrahigh-Frequency Radiation

Nashwan Abdullah[1], Bohdan Kutnyi[2], Maryna Leshchenko[3*], Liubov Shumska[4]

[1]*Poltava National Technical Yuri Kondratyuk University, Ukraine*
[2]*Poltava National Technical Yuri Kondratyuk University, Ukraine*
[3]*Poltava National Technical Yuri Kondratyuk University, Ukraine*
[4]*Poltava Oil and Gas College of Poltava National Technical Yuri Kondratyuk University, Ukraine*
**Corresponding author's E-mail: mv.leshchenko@gmail.com*

Abstract

In this work series of field experiments was conducted, a mathematical model was developed and a number of studies were performed to investigate the process of hydrate dissociation under the influence of ultrahigh-frequency radiation. The assumption is implicit that the effect of volumetric sources of heat is the dominant influence on hydration dissociation under the influence of microwave radiation, rather than the effect of boundary conditions. This provision formed the basis of the mathematical modeling of the hydrate massif dissociation. It has been established that processes of heating water, ice melting and snow, and hydrate dissociation occur in a similar way. It is characteristic that the inverse proportional dependence of internal specific heat sources on the volume of material has been obtained, that is, the decrease of the radiator efficiency when the volume of the material is reduced. It is established that volumetric thermal sources occur inside propane hydrate under the influence of microwave radiation.

Keywords: *gas hydrates, mathematical modeling, thermal conductivity, ultrahigh-frequency radiation.*

1. Introduction

During the collection, preparation, extraction, and industrial processing of gas and oil gas hydrates form in different sections of the pipelines. This leads to a decrease in the throughput capacity of the operated pipelines. In some cases they break and stop [1-5]. Therefore, elimination of hydrate formation in the extraction and transportation of oil and gas is one of the most important and significant problems [6-8]. Depositing on the inner walls of the pipes, hydrates dramatically decrease their throughput and can lead to an emergency stop of operation of the gas pipeline. Hydrates of hydrocarbon gases are unstable compounds of hydrocarbons with water and are white crystals that look like snow or ice. They consist of one or more molecules of gas (methane, propane, carbon dioxide, etc.) and water. The main factors determining the conditions for the formation of hydrates are composition of the gas, its pressure, temperature, and full saturation of gas in the water vapor.

Analytical solutions of two-dimensional nonlinear heat conduction problems are known only for certain, relatively simple cases [9-12]. The most versatile way to solve them is to apply numerical methods [13, 14], which can be easily implemented with the help of computer technology. However, numerical methods have their limitations. For example, in the method of running with the use of an implicit scheme, we have to solve a system of linear algebraic equations. The number of equations is equal to the number of nodes in the settlement grid and can be quite large. When applying an implicit scheme in the method of running, the time step is relatively small, which leads to an increase in the cost of computer time to calculate. Using the method of dynamic adaptation of networks requires a complex algorithm for implementation. Application of the average value of the coefficient of thermal conductivity on the boundary' of materials with different properties leads to changes in the thermophysical properties of materials, as a result of accumulation of errors in calculations [12, 13]. Studies of literary sources indicate the need to improve the mathematical model of non-stationary thermal regimes of two-dimensional elements in order to expand the scope of its application.

2. Main body

In order to calculate the dissociation of hydrant congestions under the conditions of microwave radiation, it is necessary to develop a digital mathematical model of non-stationary thermal modes of two-dimensional elements with necessary boundary conditions. The mathematical model should take into account the change in the thermophysical characteristics of materials, the presence of heat sources, boundary conditions, the possibility of applying variable time and coordinate steps, the absence of direct correlation between time and coordinate steps.

The basis of mathematical modeling is the Fourier's Law thermal conductivity equation with distributed volumetric heat sources, variable thermophysical characteristics of the heat conducting medium and boundary conditions of the third kind

$$c_V\rho\frac{\partial t}{\partial \tau}=\frac{\partial}{\partial x}\left(\lambda\frac{\partial t}{\partial x}\right)+\frac{\partial}{\partial y}\left(\lambda\frac{\partial t}{\partial y}\right)+q_V\,. \quad (1)$$

$$-\lambda\frac{\partial t}{\partial x}=\alpha\left(t_{(x=0,\tau)}-t_3\right)$$

$$-\lambda\frac{\partial t}{\partial y}=\alpha\left(t_{(y=0,\tau)}-t_3\right)$$

To find the temperature distribution inside a two-dimensional structure, we divide it into parallel planes on a number of layers, using the steps Δx and Δy (Fig. 1). In order to be able to apply a grid with a large number of nodes, an "explicit" scheme is required, in which at each step only one equation is solved to determine the temperature t (i, j).

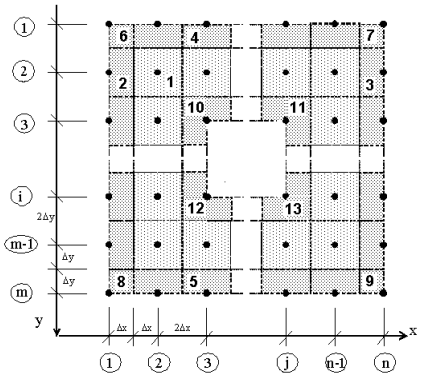

Fig. 1: Distribution of the two-dimensional structure on the internal (1), boundary (2, 3, 4, 5) and angular (6-13) elementary planes with step Δx and Δy

For internal elements of the construction (type 1), we assume that the volume of mass, limited by the step 2Δx 2Δy, is concentrated in the central point of this element. Boundary elements (2, 3, 4, 5) are located on surfaces of a two-dimensional structure, therefore only half of the mass of the inner layers is concentrated in them. The outer (6, 7, 8, 9) and inner (10, 11, 12, 13) angular elements have respectively 1/4 and 3/4 of the mass of the inner element.

Within each section of the two-dimensional design, there are evenly distributed heat sources (or heat losses) with q_V. capacity. For an internal j-th element (type 1), the differential equation of heat fluxes in finite difference can be written as follows:

$$c_{(i,j)}\rho_{(i,j)}\frac{\Delta t_{(i,j)}}{\Delta\tau}=\frac{1}{2\Delta x_{(i,j)}}\left(\frac{t_{(i,j-1)}-t_{(i,j)}}{\frac{\Delta x_{(i,j-1)}}{\lambda_{(i,j-1)}}+\frac{\Delta x_{(i,j)}}{\lambda_{(i,j)}}}-\frac{t_{(i,j)}-t_{(i,j+1)}}{\frac{\Delta x_{(i,j)}}{\lambda_{(i,j)}}+\frac{\Delta x_{(i,j+1)}}{\lambda_{(i,j+1)}}}\right)+, \quad (2)$$

$$+\frac{1}{2\Delta y_{(i,j)}}\times\left(\frac{t_{(i-1,j)}-t_{(i,j)}}{\frac{\Delta y_{(i-1,j)}}{\lambda_{(i-1,j)}}+\frac{\Delta y_{(i,j)}}{\lambda_{(i,j)}}}-\frac{t_{(i,j)}-t_{(i+1,j)}}{\frac{\Delta y_{(i,j)}}{\lambda_{(i,j)}}+\frac{\Delta y_{(i+1,j)}}{\lambda_{(i+1,j)}}}\right)+q_{V(i,j)}$$

where $c_{(i,j)}$ – is the heat capacity of material of the enclosing structure, J/ kg°C;

$\rho_{(i,j)}$ is the material density of the heat accumulation platform, kg/m^3;

$t_{(i,j)}$ is the platform temperature of a two-dimensional structure with coordinates X=i, Y=j, °C;

$\Delta\tau$ is the estimated time interval, sec;

$\lambda_{(i,j)}$ is the thermal conductivity of the material, W / m°C;

Δx, Δy are coordinate steps correspondingly along the X axis and Y axis, m;

$q_{V(i,j)}$ is the specific volume heat source, W / m^3.

For the two-dimensional task, the boundary conditions have their own peculiarities. First, their number is equal to the number of lines that limit the calculation area. They limit both external and internal surface design. Secondly, the boundary conditions can vary along the axis for which they are given. If the third-generation boundary conditions are set near the external surface of the calculated area, then the heat balance equation for the first layer (element 2) will look like this:

$$c_{(i,j)}\rho_{(i,j)}\frac{\Delta t_{(i,j)}}{\Delta\tau}=\frac{1}{\Delta x_{(i,j)}}\left(\alpha_{(i,j)}\left(t_{o(i,j)}-t_{(i,j)}\right)-\frac{t_{(i,j)}-t_{(i,j+1)}}{\frac{\Delta x_{(i,j)}}{\lambda_{(i,j)}}+\frac{\Delta x_{(i,j+1)}}{\lambda_{(i,j+1)}}}\right)+, \quad (3)$$

$$+\frac{1}{2\Delta y_{(i,j)}}\times\left(\frac{t_{(i-1,j)}-t_{(i,j)}}{\frac{\Delta y_{(i-1,j)}}{\lambda_{(i-1,j)}}+\frac{\Delta y_{(i,j)}}{\lambda_{(i,j)}}}-\frac{t_{(i,j)}-t_{(i+1,j)}}{\frac{\Delta y_{(i,j)}}{\lambda_{(i,j)}}+\frac{\Delta y_{(i+1,j)}}{\lambda_{(i+1,j)}}}\right)+q_{V(i,j)}$$

where $\alpha_{(i,j)}$ is the local heat transfer coefficient near the corresponding element of the surface, W / (m2 °C);

$t_{0(i,j)}$ is the environment temperature, washing the local element of the surface, °C.

Similarly, the boundary conditions (heat exchange of a gaseous medium with outer layers) can be written for other three sides of the rectangular area (elements 3, 4, 5)

$$c_{(i,j)}\rho_{(i,j)}\frac{\Delta t_{(i,j)}}{\Delta\tau}=\frac{1}{\Delta x_{(i,j)}}\left(\frac{t_{(i,j-1)}-t_{(i,j)}}{\frac{\Delta x_{(i,j-1)}}{\lambda_{(i,j-1)}}+\frac{\Delta x_{(i,j)}}{\lambda_{(i,j)}}}-\alpha_{(i,j)}\left(t_{(i,j)}-t_{o(i,j)}\right)\right)+,$$

$$\frac{1}{2\Delta y_{(i,j)}}\times\left(\frac{t_{(i-1,j)}-t_{(i,j)}}{\frac{\Delta y_{(i-1,j)}}{\lambda_{(i-1,j)}}+\frac{\Delta y_{(i,j)}}{\lambda_{(i,j)}}}-\frac{t_{(i,j)}-t_{(i+1,j)}}{\frac{\Delta y_{(i,j)}}{\lambda_{(i,j)}}+\frac{\Delta y_{(i+1,j)}}{\lambda_{(i+1,j)}}}\right)+q_{V(i,j)}$$

$$c_{(i,j)}\rho_{(i,j)}\frac{\Delta t_{(i,j)}}{\Delta\tau}=\frac{1}{2\Delta x_{(i,j)}}\left(\frac{t_{(i,j-1)}-t_{(i,j)}}{\frac{\Delta x_{(i,j-1)}}{\lambda_{(i,j-1)}}+\frac{\Delta x_{(i,j)}}{\lambda_{(i,j)}}}-\frac{t_{(i,j)}-t_{(i,j+1)}}{\frac{\Delta x_{(i,j)}}{\lambda_{(i,j)}}+\frac{\Delta x_{(i,j+1)}}{\lambda_{(i,j+1)}}}\right)+, \quad (4)$$

$$\frac{1}{\Delta y_{(i,j)}}\times\left(\alpha_{(i,j)}\left(t_{o(i,j)}-t_{(i,j)}\right)-\frac{t_{(i,j)}-t_{(i+1,j)}}{\frac{\Delta y_{(i,j)}}{\lambda_{(i,j)}}+\frac{\Delta y_{(i+1,j)}}{\lambda_{(i+1,j)}}}\right)+q_{V(i,j)}$$

$$c_{(i,j)}\rho_{(i,j)}\frac{\Delta t_{(i,j)}}{\Delta\tau}=\frac{1}{2\Delta x_{(i,j)}}\left(\frac{t_{(i,j-1)}-t_{(i,j)}}{\frac{\Delta x_{(i,j-1)}}{\lambda_{(i,j-1)}}+\frac{\Delta x_{(i,j)}}{\lambda_{(i,j)}}}-\frac{t_{(i,j)}-t_{(i,j+1)}}{\frac{\Delta x_{(i,j)}}{\lambda_{(i,j)}}+\frac{\Delta x_{(i,j+1)}}{\lambda_{(i,j+1)}}}\right)+.$$

$$\frac{1}{\Delta y_{(i,j)}}\times\left(\frac{t_{(i-1,j)}-t_{(i,j)}}{\frac{\Delta y_{(i-1,j)}}{\lambda_{(i-1,j)}}+\frac{\Delta y_{(i,j)}}{\lambda_{(i,j)}}}-\alpha_{(i,j)}\left(t_{(i,j)}-t_{o(i,j)}\right)\right)+q_{V(i,j)}$$

In addition to the linear boundaries on the calculated plane, there are also angular elements, which are characterized by the simultaneous action of boundary conditions on two coordinate axes. Angular elements can be divided into "external" and "internal". External elements (type 6, 7, 8, 9) touch only the boundary elements of the calculated plane (Fig. 1), therefore their thermal regime can be described by the equations of the

form:

$$c_{(i,j)}\rho_{(i,j)}\frac{\Delta t_{(i,j)}}{\Delta\tau}=\frac{1}{\Delta x_{(i,j)}}\left(\alpha_{(i,j)}\left(t_{o(i,j)}-t_{(i,j)}\right)-\frac{t_{(i,j)}-t_{(i,j+1)}}{\frac{\Delta x_{(i,j)}}{\lambda_{(i,j)}}+\frac{\Delta x_{(i,j+1)}}{\lambda_{(i,j+1)}}}\right)+$$

$$\frac{1}{\Delta y_{(i,j)}}\times\left(\alpha_{(i,j)}\left(t_{o(i,j)}-t_{(i,j)}\right)-\frac{t_{(i,j)}-t_{(i+1,j)}}{\frac{\Delta y_{(i,j)}}{\lambda_{(i,j)}}+\frac{\Delta y_{(i+1,j)}}{\lambda_{(i+1,j)}}}\right)+q_{V(i,j)}$$

$$c_{(i,j)}\rho_{(i,j)}\frac{\Delta t_{(i,j)}}{\Delta\tau}=\frac{1}{\Delta x_{(i,j)}}\left(\frac{t_{(i,j-1)}-t_{(i,j)}}{\frac{\Delta x_{(i,j-1)}}{\lambda_{(i,j-1)}}+\frac{\Delta x_{(i,j)}}{\lambda_{(i,j)}}}-\alpha_{(i,j)}\left(t_{(i,j)}-t_{o(i,j)}\right)\right)+$$

$$\frac{1}{\Delta y_{(i,j)}}\times\left(\alpha_{(i,j)}\left(t_{o(i,j)}-t_{(i,j)}\right)-\frac{t_{(i,j)}-t_{(i+1,j)}}{\frac{\Delta y_{(i,j)}}{\lambda_{(i,j)}}+\frac{\Delta y_{(i+1,j)}}{\lambda_{(i+1,j)}}}\right)+q_{V(i,j)}$$

$$c_{(i,j)}\rho_{(i,j)}\frac{\Delta t_{(i,j)}}{\Delta\tau}=\frac{1}{\Delta x_{(i,j)}}\left(\alpha_{(i,j)}\left(t_{o(i,j)}-t_{(i,j)}\right)-\frac{t_{(i,j)}-t_{(i,j+1)}}{\frac{\Delta x_{(i,j)}}{\lambda_{(i,j)}}+\frac{\Delta x_{(i,j+1)}}{\lambda_{(i,j+1)}}}\right)+ \quad (5)$$

$$\frac{1}{\Delta y_{(i,j)}}\times\left(\frac{t_{(i-1,j)}-t_{(i,j)}}{\frac{\Delta y_{(i-1,j)}}{\lambda_{(i-1,j)}}+\frac{\Delta y_{(i,j)}}{\lambda_{(i,j)}}}-\alpha_{(i,j)}\left(t_{(i,j)}-t_{o(i,j)}\right)\right)+q_{V(i,j)}$$

$$c_{(i,j)}\rho_{(i,j)}\frac{\Delta t_{(i,j)}}{\Delta\tau}=\frac{1}{\Delta x_{(i,j)}}\left(\frac{t_{(i,j-1)}-t_{(i,j)}}{\frac{\Delta x_{(i,j-1)}}{\lambda_{(i,j-1)}}+\frac{\Delta x_{(i,j)}}{\lambda_{(i,j)}}}-\alpha_{(i,j)}\left(t_{(i,j)}-t_{o(i,j)}\right)\right)+$$

$$\frac{1}{\Delta y_{(i,j)}}\times\left(\frac{t_{(i,j)}-t_{(i+1,j)}}{\frac{\Delta y_{(i,j)}}{\lambda_{(i,j)}}+\frac{\Delta y_{(i+1,j)}}{\lambda_{(i+1,j)}}}-\alpha_{(i,j)}\left(t_{(i,j)}-t_{o(i,j)}\right)\right)+q_{V(i,j)}$$

To specify any form of heat exchange area internal nodes must be taken into account. Such nodes will also be species (10, 11, 12, 13). Equations for the description of heat exchangers processes in such nodes have the form:

$$c_{(i,j)}\rho_{(i,j)}\frac{\Delta t_{(i,j)}}{\Delta\tau}=\frac{1}{3\Delta x_{(i,j)}}\left(\frac{t_{(i,j-1)}-t_{(i,j)}}{\frac{\Delta x_{(i,j-1)}}{\lambda_{(i,j-1)}}+\frac{\Delta x_{(i,j)}}{\lambda_{(i,j)}}}-\alpha_{(i,j)}\left(t_{(i,j)}-t_{o(i,j)}\right)-\frac{2\left(t_{(i,j)}-t_{(i,j+1)}\right)}{\frac{\Delta x_{(i,j)}}{\lambda_{(i,j)}}+\frac{\Delta x_{(i,j+1)}}{\lambda_{(i,j+1)}}}\right)+$$

$$+\frac{1}{3\Delta y_{(i,j)}}\times\left(\frac{2\left(t_{(i-1,j)}-t_{(i,j)}\right)}{\frac{\Delta y_{(i-1,j)}}{\lambda_{(i-1,j)}}+\frac{\Delta y_{(i,j)}}{\lambda_{(i,j)}}}-\alpha_{(i,j)}\left(t_{(i,j)}-t_{o(i,j)}\right)-\frac{t_{(i,j)}-t_{(i+1,j)}}{\frac{\Delta y_{(i,j)}}{\lambda_{(i,j)}}+\frac{\Delta y_{(i+1,j)}}{\lambda_{(i+1,j)}}}\right)+q_{V(i,j)}$$

$$c_{(i,j)}\rho_{(i,j)}\frac{\Delta t_{(i,j)}}{\Delta\tau}=\frac{1}{3\Delta x_{(i,j)}}\left(\frac{2\left(t_{(i,j-1)}-t_{(i,j)}\right)}{\frac{\Delta x_{(i,j-1)}}{\lambda_{(i,j-1)}}+\frac{\Delta x_{(i,j)}}{\lambda_{(i,j)}}}-\alpha_{(i,j)}\left(t_{(i,j)}-t_{o(i,j)}\right)-\frac{t_{(i,j)}-t_{(i,j+1)}}{\frac{\Delta x_{(i,j)}}{\lambda_{(i,j)}}+\frac{\Delta x_{(i,j+1)}}{\lambda_{(i,j+1)}}}\right)+ \quad (6)$$

$$+\frac{1}{3\Delta y_{(i,j)}}\times\left(\frac{t_{(i-1,j)}-t_{(i,j)}}{\frac{\Delta y_{(i-1,j)}}{\lambda_{(i-1,j)}}+\frac{\Delta y_{(i,j)}}{\lambda_{(i,j)}}}-\alpha_{(i,j)}\left(t_{(i,j)}-t_{o(i,j)}\right)-\frac{2\left(t_{(i,j)}-t_{(i+1,j)}\right)}{\frac{\Delta y_{(i,j)}}{\lambda_{(i,j)}}+\frac{\Delta y_{(i+1,j)}}{\lambda_{(i+1,j)}}}\right)+q_{V(i,j)}$$

Thus, we have obtained a system of equations (2-6) with the corresponding number of unknown temperatures. To increase the time step of the given system of equations is convenient to solve using the Runge-Kutta digital method of the 4th order. All its coefficients (α, λ, α, λ, c, ρ, qv) can be defined as functions coordinates, temperature and temperature difference. In addition, its feature is the possibility of breaking the design to the desired number of layers, variable grid density and no rigidity link of coordinate and time steps.

High-frequency electromagnetic waves that propagate along the coaxial transmission line, lose their own capacity due to losses in the metal wall of the pipe and in dielectric (hydrate) that fills the inside space. The distribution density of heat sources is determined by the expression

$$q=-\frac{1}{2}\mathrm{Re}\frac{\partial}{\partial z}\left(\overset{\bullet}{E_r}\cdot\overset{\bullet}{H_\varphi}\right). \quad (7)$$

As seen from expression (7), the density of heat sources created in the environment that interacts with the electromagnetic field (EMF) is also a function of the electric field tension. Distribution EMF tension depends, first of all, on the geometry of the system and the device in which the EMF is created (free space, coaxial system, waveguide and resonator).

Components of the intensity of the electromagnetic field are determined from solutions of the Maxwell equations by formulas

$$\overset{\bullet}{E}_{0r}=\frac{\dot{D}}{r}\ell^{-j\Gamma Z}, \quad (8)$$

$$\overset{\bullet}{H}_{0\varphi}=\frac{\overset{\bullet}{E}_{0r}}{\dot{Z}_C}=\frac{\dot{D}}{\dot{Z}_C r}\ell^{-j\Gamma Z}, \quad (9)$$

Where, $\dot{D}$ is the complex amplitude of an electromagnetic wave;

$\dot{Z}_C$ is the dielectric resistance, which fills the space of pipeline, Ohm. It can be defined by the formula

$$\dot{Z}_C=\sqrt{\frac{\mu_0}{\varepsilon_0\varepsilon}}\left(1+0.5jtg\delta\right), \quad (10)$$

ε' is the relative dielectric permittivity of the dielectric, which fills the space of the pipeline;

ε_0, μ_0 – are dielectric and magnetic permeability of vacuum, F / m and GN / m. Dielectric vacuum permeability $\varepsilon_0=8{,}8542\cdot10^{-12}$ F/m

$\dot{\Gamma}$ is the constant propagation of electromagnetic waves, which is determined by $\dot{\Gamma}=\beta-j\alpha$, m^{-1};

β is the wave number, m^{-1};

j is the imaginary unit;

α is the damping coefficient of electromagnetic waves, m^{-1}.

Substituting instead $\overset{\bullet}{E}_{0r}$ and $\overset{\bullet}{H}_{0\varphi}$ their expressions from (8) to (9), we will get

$$q = \frac{\alpha \left|\dot{D}\right|^2}{r^2 Z} \ell^{-2\alpha Z}. \quad (11)$$

To find the unknown value of $\dot{D}$ we have correlation

$$\left|\dot{D}\right|^2 = \frac{2r^2 Z_c P_0}{\pi R^2}. \quad (12)$$

Taking into account formula (12), we obtain an expression for calculating the capacity of local sources

$$q = \frac{2\alpha P_0}{\pi R^2} \ell^{-2\alpha Z}. \quad (13)$$

Heat treatment of pipeline round section with heat sources in the form of microwave radiation is calculated by the formula

$$\rho c \frac{\partial T}{\partial t} = \frac{\partial}{\partial r}\left(\lambda r \frac{\partial T}{\partial r}\right) + \frac{2\alpha P_0}{\pi R^2} \ell^{-2\alpha z}, \quad (14)$$

where, ρ is the material density, kg/m3;
c is the heat capacity of the material, J/(kg C);
P_0 is the input capacity, W
Distance from the point of entry of radiation to the calculated plot is determined by the formula

$$z = \sqrt{x^2 + y^2}, \quad (15)$$

where x, y – are distance from the radiation source to the calculation points, m.
Total coefficient of electromagnetic waves damping consists of two parts

$$\alpha = \alpha_\Gamma + \alpha_{TP}, \quad (16)$$

where α_Γ are damping coefficient of electromagnetic waves of hydrate;

α_{TP} is the damping coefficient of electromagnetic waves in the pipeline.
Attenuation coefficient in the pipeline is

$$\alpha_{TP} = \frac{R_{S3}}{2 Z_e R_2 \ln(R_3 / R_2)}. \quad (17)$$

The value of R_{S3} is found by the formula

$$R_{S3} = \sqrt{\frac{\pi f \mu_{a3}}{\sigma_3}}, \quad (18)$$

where f – is the frequency, Hz;

μ_{a3} is the absolute magnetic permeability of the pipeline, Gn/m;

σ_3 is specific electrical conductivity of a steel pipeline, $Ohm^{-1} \cdot m^{-1}$.
Therefore,

$$\alpha_{TP} = \sqrt{\frac{\pi f \mu\mu_0}{\sigma}} \times \frac{1}{Z_c R_{TP} \sqrt{1 - \left(\frac{\lambda_0}{\lambda_{kp}}\right)^2}}, \quad (19)$$

where μ_0 is the magnetic permeability of vacuum;

$Z_c = \sqrt{\frac{\mu_0}{\varepsilon_0}}$ is the wave impedance of the dielectric filling the pipeline, Ohm.
Frequency of electromagnetic oscillations of the emitter is f=2.45·10^{9}Hz. The magnetic permeability of the vacuum is μ_0=1,2566·10^{-6} Gn / m. Relative magnetic permeability of the steel pipe is μ = 2,72 Gn/m. Conductivity of the pipeline is σ=0,34·107 $Ohm^{-1} \cdot m^{-1}$.
Substituting known values, we obtain, Ohm

$$Z_c = \sqrt{\frac{\mu_0}{\varepsilon_0}} = \sqrt{\frac{1.2566 \cdot 10^{-6}}{8.8542 \cdot 10^{-12}}} \approx 377.$$

To hydrate, the attenuation coefficient is determined by the formula

$$\alpha_\Gamma = \frac{\pi \varepsilon' tg\delta}{\lambda_0 \sqrt{1 - \frac{1}{\varepsilon'}\left(\frac{\lambda_0}{\lambda_{kp}}\right)^2}}. \quad (20)$$

Characteristic values for hydrate are ε' =3,75 and tgδ=0,02.

$$\lambda_0 = \frac{1,841}{2\pi R_{Tp}} \frac{1}{\sqrt{\varepsilon_0 \mu_0}}. \quad (21)$$

The origin of internal heat sources in such a dielectric in the interaction with microwave EMF and, consequently, temperature change and pressure can create a method of decomposition of gas hydrates using the energy of microwave EMF

The example of the above can be calculating of specific volumetric heat consumption from microwave radiation for pipeline diameter 100 mm.

Consumer power of the radiator is 1000W, efficiency is 50%. Critical wave length is

$$\lambda_{kp} = \frac{\pi D_{Tp}}{S_{mn}} = \frac{2\pi R_{Tp}}{S_{mn}} = \frac{3,1415 \cdot 10}{1,841} = 17,06$$

where S_{mn}=1,841 is mode TE11.
For the frequency at which the microwave emitter (magnetron) f_0=2,45·109 Hz, the wavelength is, cm

$$\lambda_0 = \frac{c}{f_0} = \frac{3 \cdot 10^{10}}{2,45 \cdot 10^9} = 12,24,$$

where c is the speed of light c=300·10^6 m / s, or c=3·10^{10} cm / sec. So the condition is satisfied $\lambda_0 < \lambda_{kp}$. The square of the ratio of wave lengths is

$$\left(\frac{\lambda_0}{\lambda_{kp}}\right)^2 = \left(\frac{12,24}{17,06}\right)^2 = (0,717)^2 = 0,515.$$

Substituting the values in formula (20), we determine radiation damping coefficient for hydrate

$$\alpha_{\Gamma} = \frac{3{,}1415 \cdot 3{,}75 \cdot 0{,}02}{0{,}1224\sqrt{1-\frac{1}{3{,}75}\cdot 0{,}515}} = 0{,}207.$$

Coefficient of attenuation in a steel pipeline radius 0,05 m

$$\alpha_{TP} = \sqrt{\frac{3{,}1415 \cdot 2{,}45 \cdot 10^{9} \cdot 2{,}72 \cdot 1{,}2566 \cdot 10^{-6}}{0{,}34 \cdot 10^{7}}} \times \frac{1}{377 \cdot 0{,}05 \cdot \sqrt{1-0{,}515}} =$$

$$= 0{,}0067.$$

Thus, the damping coefficient of electromagnetic waves in the pipeline is α_{TP}= 0,0067. The total damping factor is α=0,207+0,0067=0,2137.

The sources of heat in hydrate are determined by the formula

$$q_{\Gamma} = \frac{2 \cdot 0{,}207 \cdot P_0}{3{,}1415 \cdot 0{,}05^2} \ell^{-2 \cdot 0{,}2137 \cdot z}.$$

Taking into account the capacity P_0= 1000 0,5 = 500 W, the sources of heat in the pipeline are determined by the formula

$$q_{TP} = \frac{2 \cdot 0{,}0067 \cdot 500}{3{,}1415 \cdot 0{,}05^2} \ell^{-2 \cdot 0{,}2137 \cdot z} = 853\ell^{-0{,}4274 \cdot z}.$$

Sources of heat in gas hydrate are calculated as follows

$$q_{\Gamma} = \frac{2 \cdot 0{,}207 \cdot 500}{3{,}1415 \cdot 0{,}05^2} \ell^{-2 \cdot 0{,}2137 \cdot z} = 26357\ell^{-0{,}4274 \cdot z}.$$

The proposed mathematical model is used to create a computer program in the language of QBasic. The code size is 9.5 kilobytes. The proposed digital mathematical model can be used for calculating transitional heat transfer processes in two-dimensional elements of constructions, taking into account changes in physical properties of a material (dissociation of hydrate), heat sources in the form of heat transfer from microwave radiation and heat losses to dissociation of hydrate and boundary conditions of the third kind. For its solution, the Runge-Kutta method of the 4th order is used.

2.1. Experimental research on hydrate dissociation under the action of ultrahigh-frequency radiation

An experimental installation was designed for experimental research. Constructive scheme is constructed shown in Figure 2.

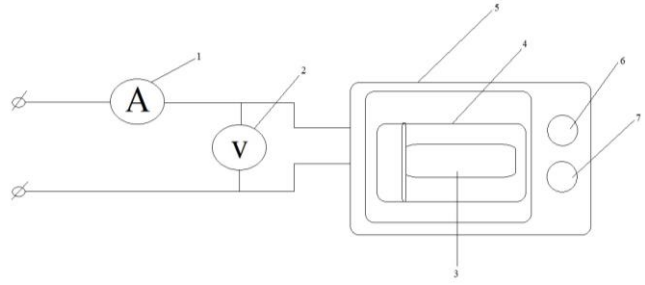

Fig. 2: Scheme of experimental setup for decomposition of nitrate by microwave radiation:1 – ammeter; 2 – voltmeter; 3 – hydrate; 4 – atransparent bulb; 5 – microwave oven; 6 – time control button; 7 – mode adjustment button

To study the hydrate decomposition in a closed volume in pilot glass is filled with hydrate, the lid is hermetically sealed and microwave emitter is switched on (Fig. 3).

The laboratory installation for decomposition of the gas hydrate works as follows. The propane hydrate obtained for researches is stored in a sealed steel container in a freezing chamber at a temperature from minus 10 ºC to minus 15 ºC. You should get the required amount of hydrate, pour it into a transparent bulb and seal hermetically. The transparent bulb is placed in a laboratory plant with a high-frequency emitter and switched on at a given time and mode. In every 5 seconds, a transparent bulb is removed and visually evaluated when the hydration portion is decomposed. During each ejection, the temperature and the amount of water formed is measured by means of electronic weights. If the process of decomposition of hydrate does not take place, the transparent bulb is placed back into the laboratory plant, and a new time of irradiation of the EMF is given. This procedure is repeated until all of the hydrate is decomposed. At the same time the result of the decomposition of hydrate is recorded in the corresponding table of the laboratory journal.

Fig. 3: General view of the test glass inside the laboratory installation of the microwave emitter

To determine the capacity of heat sources and the UHF efficiency heating with the help of EMF a series of experiments was carried out, such us water heating, ice melting and snow, hydration decomposition propane under atmospheric pressure.

Dependencies (22) – (23) were applied to process the received experimental data.

The amount of energy absorbed by the microwave emitter from alternating voltage network, J.

$$N = U \cdot I \cdot z, \quad (22)$$

where U is the network voltage, V;
I is the current, A;
z is the time, sec.

The amount of heat used to heat water, J.

$$Q_в = M \cdot c \cdot (t_2 - t_1), \quad (23)$$

where M is the weight of water, kg;
c=4187 is the mass heat capacity of water, J/(kg °C);
t_2 is the final temperature, °C;
t_1 is the initial temperature, °C.

The amount of heat used to make phase transformations, J.

$$Q_ф = m \cdot r, \quad (24)$$

where m is the weight of the substance that carried out the phase transition, kg;
r is the heat of the phase transition, J/kg

The volume of substance, which is affected by microwave radiation, m^3, is

$$V = M/\rho, \quad (25)$$

where ρ is the density of the substance, kg / m^3.

Specific power of bulk sources of microwave energy, W / m^3, is calculated by the formula

$$q_v = (Q_ф + Q_в)/z/V. \quad (26)$$

The coefficient of efficiency of the installation is determined by the formula (27), %.

Energy efficiency equals

$$(Q_ф + Q_в)/N \cdot 100. \quad (27)$$

Before the start of the main series of studies, it was necessary to make sure that the volumetric sources of heat, but not the boundary conditions on the surface, played the key role in the heating processes of the substances being investigated.

The purpose of the next study was to determine the degree of influence of the shape of ice (or hydrate) on the power of heat sources. For this purpose, a cylindrical piece of ice with a surface area of F = 0,0086 m^2 and an ice plate with a thickness of 4,3 mm with a surface F = 0,048 m^2 were heated. The results of the experiment to determine the mechanism of influence of microwave radiation are presented in Table 1. Average values of the obtained indicators and their ratios are shown in Tables 2 and 3, respectively.

Table 1: Results of laboratory tests for determining the mechanism of microwave radiation influence

t_1	t_2	time	mass	F	Q	V	q_v
°C	°C	sec	g	m^2	kJ	m^3	W/m^3
0	50	60	50	0,0086	26,97	5,28148E-05	8510
0	23	50	50	0,0086	21,32	5,28148E-05	8072
0	45	55	50	0,0086	25,92	5,28148E-05	8923
0	32	53	50	0,0086	23,20	5,28148E-05	8288
0	29	51	50	0,0086	22,57	5,28148E-05	8380
0	26	50	50	0,0086	21,94	5,28148E-05	8309
0	42	59	50	0,0086	25,29	5,28148E-05	8117
0	30	103	100	0,048	45,56	0,0001032	4286
0	28	101	100	0,048	44,72	0,0001032	4291
0	34	107	100	0,048	47,24	0,0001032	4278
0	50	115	100	0,048	53,94	0,0001032	4545
0	45	109	100	0,048	51,84	0,0001032	4609
0	36	108	100	0,048	48,07	0,0001032	4313
0	31	105	100	0,048	45,98	0,0001032	4243

Table 2: Average values of the obtained indicators

t_1	t_2	time	mass	F	Q	V	q_v
°C	°C	sec	g	m^2	kJ	m^3	W/m^3
0	35,3	54,0	0,05	0,0086	23,9	0,0000528	8371,3
0	36,3	106,9	0,1	0,0480	48,2	0,0001032	4366,3

Table 3: Correlation of average values of the obtained indicators

t_1	t_2	time	mass	F	Q	V	q_v
°C	°C	sec	g	m^2	kJ	m^3	W/m^3
1	1,028	1,979	2,000	5,576	2,018	1,954	0,522

The results of experimental studies have shown that when constant heat transfer conditions increase sample volume twice it leads to twofold a reduction of specific volumetric sources. Increase in the surface area in 5.6 times does not affect the power of heat sources. The experiment confirms that the effect of microwave radiation is first of all volumetric rather than superficial. Therefore, all further research is primarily aimed at the establishing the dependence of volumetric heat sources on the influence of various factors.

2.2. Series of experimental studies: water heating

Based on the results of experimental studies we designed the graph of the dependence of heat sources on the volume of water (Fig. 4) and effect of the emitter (Fig. 5). Analysis of graphs allows concluding that the specific power of heat sources is inversely proportional to the amount of water. At the volume of material more than 0.5 liters, the specific power is on the constant level and makes 0,83 kW/l with less quantity material than 0.5 liters, there is an increase in intensity sources, which can reach 3.5 kW / l. Research in the efficiency of emitter indicates the value of 60 ÷ 70% within the volume 0,3-1 l. For small volumes, the decrease in efficiency up to 13-14% is characteristic.

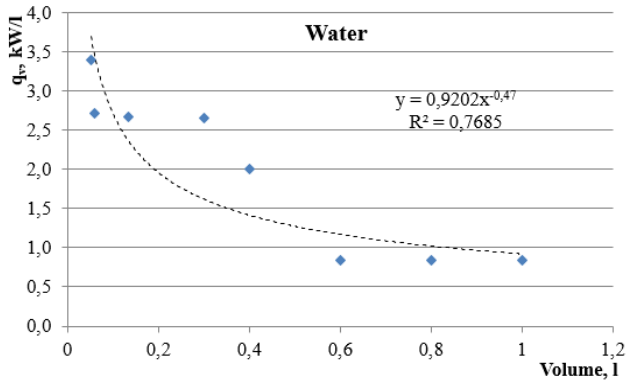

Fig. 4: Dependence of the specific power of internal heat sources on the water volume

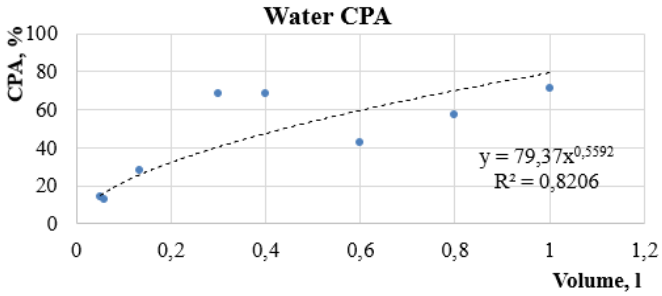

Fig. 5: Dependence of the emitter efficiency on the water volume

2.3. Series of experimental studies: ice melting

According to its thermophysical properties, ice is similar to hydrate. Therefore, a series of studies was conducted to determine the efficiency of the emitter and the intensity of internal heat sources for ice samples of different volumes.

The results of data processing for different initial masses of ice are presented in the form of charts in Figures 6 and 7. The average value of specific volumetric sources for the whole series is shown in Figure 10. The average value of the efficiency of the emitter for the whole series is shown in Figure 11.

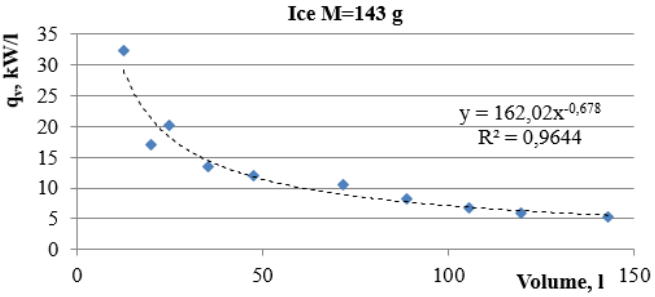

Fig. 6: The intensity of internal sources in the process of the ice melting with the initial weight of 143 g

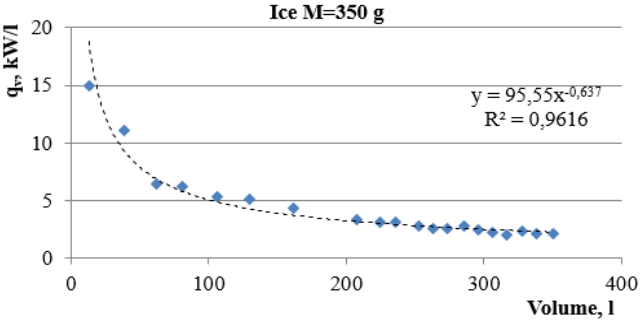

Fig. 7: The intensity of internal sources in the process of the ice melting with the initial weight of 350 g

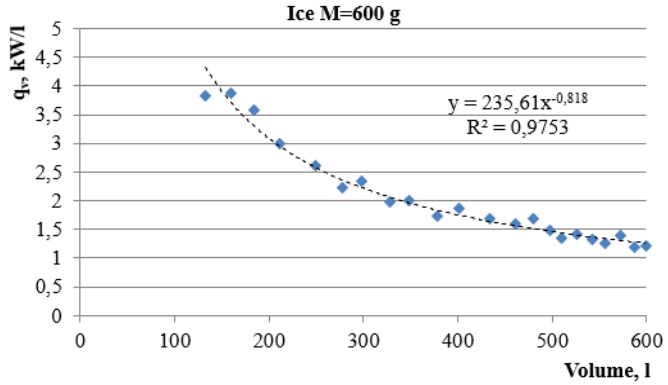

Fig. 8: The intensity of internal sources in the process of the ice melting with the initial weight of 600 g

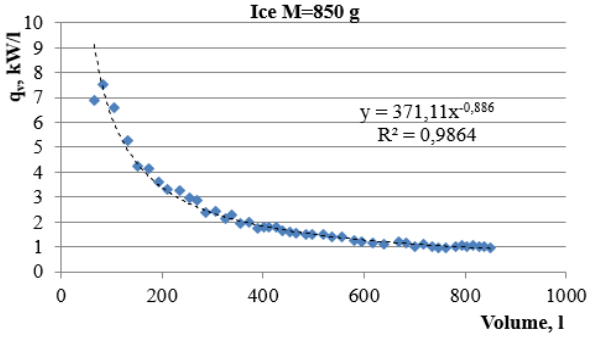

Fig. 9: The intensity of internal sources in the process of the ice melting with the initial weight of 850 g

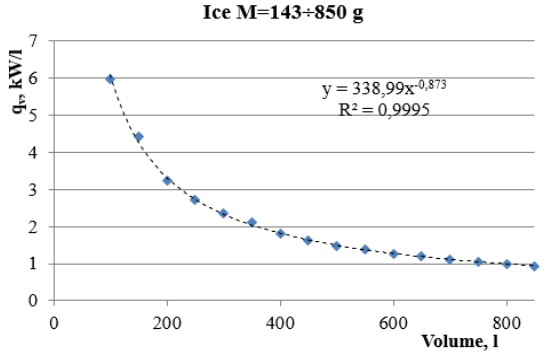

Fig. 10: The average intensity of internal sources during the ice melting with the initial weight of 143÷850 g

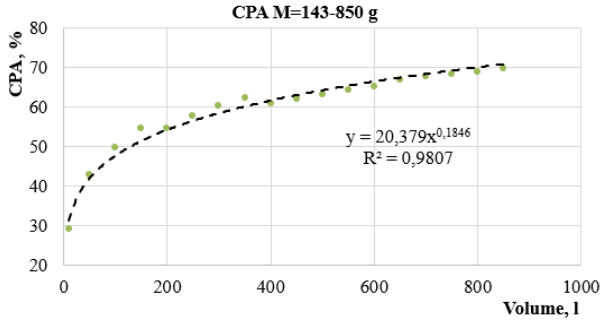

Fig. 11: The efficiency of the emitter in conditions of ice melting with an initial weight of 143-850 g

The results of experimental studies have shown that in the case of melting of ice under the influence of microwave radiation, the intensity of heat sources is an inverse function to the mass of ice. The efficiency of the emitter increases as the mass of ice increases as well.

2.4. Series of experimental studies: snow melting

The volumetric density of hydrate is often similar to the density of snow. Therefore, this series of experimental studies was carried out to determine the influence of gas layers in the mass of the material on the intensity of internal heat sources. For experimental research, snow of natural origin with a density of 480 ÷ 640 kg / m^3 was used. The results of the performed research are presented in the graphs in Figures 12-15.

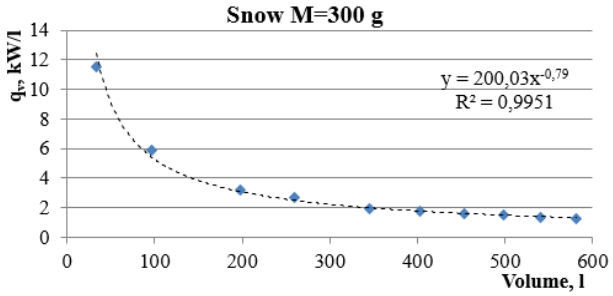

Fig. 12: The intensity of internal sources during the melting of the initial snow weight of 300 g

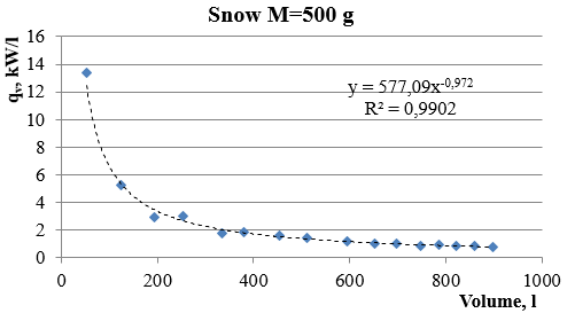

Fig. 13: The intensity of internal sources during the melting of the initial snow weight of 500 g

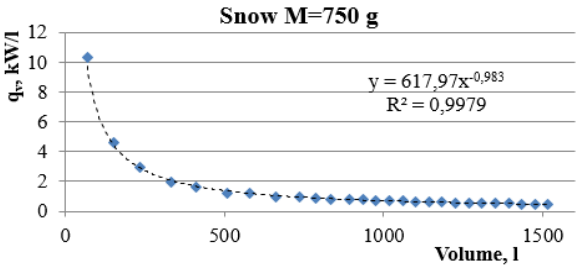

Fig. 14: The intensity of internal sources during the melting of the initial snow weight of 750 g

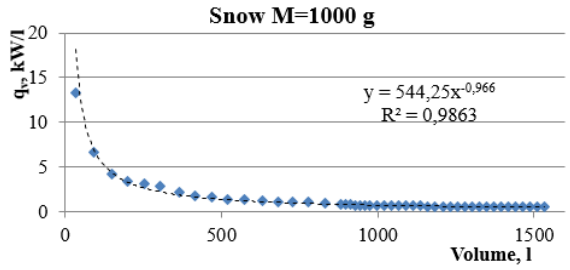

Fig. 15: The intensity of internal sources during the melting of the initial snow weight of 1000 g

The average intensity of internal heat sources for snow weight from 300 to 1000 g is graphically shown in Figure 16.

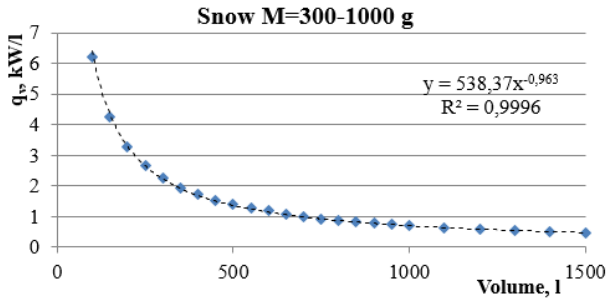

Fig. 16: The average intensity of internal sources during melting of snow with an initial weight of 300-1000 g

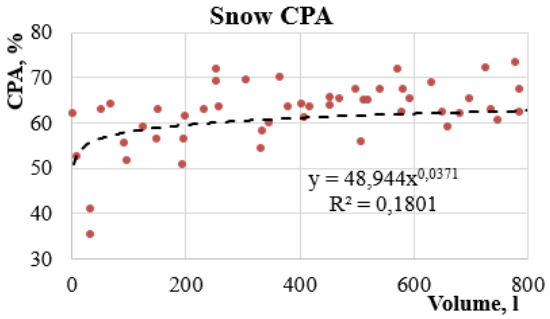

Fig. 17: Emitter efficiency in terms of melting snow weighing 300-1000 g

The results of experimental studies have shown that in the case of melting of snow under the influence of microwave radiation, the intensity of heat sources is a reversed function to the mass of snow. The efficiency of the radiator varies little with the change in the mass of snow. Its average value is 62%.

2.5. Series of experimental studies: propane hydrate dissociation

To study the dissociation of hydrate in the conditions of microwave radiation, propane hydrate was used. Studies were conducted for different volumes of hydrate. The results of determining the power of internal sources for four experiments with a small amount of hydrate (15.55 - 27.67 g) are shown graphically in Figure 18.

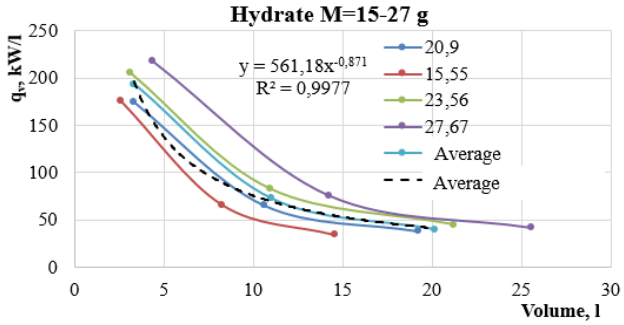

Fig. 18: The intensity of internal sources during propane hydrate dissociation with initial weight from 15.55 to 27.67 g

The obtained results show that the reduction of the initial volume of hydrate leads to a decrease in the intensity of specific volumetric sources of thermal energy (q_v). At the same time, q_v is an inverse function to the amount of remaining hydrate. On the basis of experimental data, the average value of q_v is determined and the approximation function is obtained, kW / l

$$q_v = \frac{561.18}{V_g^{0.871}}. \quad (28)$$

Dissociation of a specimen weighing 90 g was performed to verify the obtained dependence on larger volumes of hydrate. The results of the measurements are shown graphically in Figures 19 and 20.

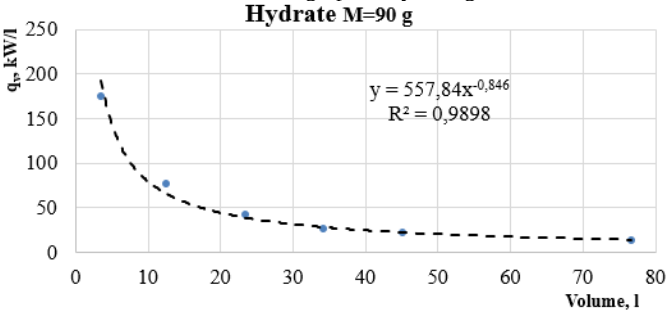

Fig. 19: The intensity of internal sources for propane hydrate of 90 g

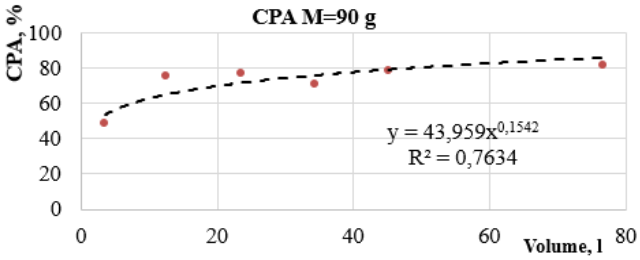

Fig. 20: Efficiency of the hydrate decomposition with an initial weight of 90 g

The obtained results indicate a greater intensity of volumetric heat sources for hydrate, snow, ice and water. The efficiency of the energy of the electromagnetic field of the magnetron also increased to 80%.

The following series of experimental studies was conducted with an increased amount of hydrate. The results of determining specific volumetric heat sources are shown graphically in Figures 21 and 22.

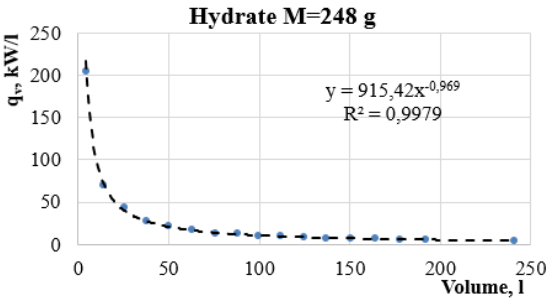

Fig. 21: The intensity of internal sources for propane hydrate of 248 g

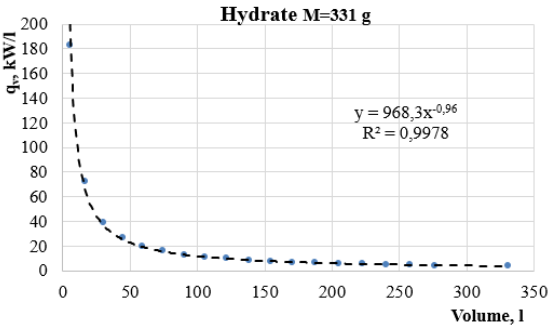

Fig. 22: The intensity of internal sources for propane hydrate of 331 g

The graph in Figure 23 shows that, for both ice and snow, the use of microwave radiation efficiency depends on the amount of

hydrate. However, higher energy absorption efficiency than ice and snow is 80-92% for large amounts of hydrate.
To compare the main characteristics of the microwave radiation processes of various substances (water, snow, ice and hydrate), all approximating curves are shown on the plotted graph (Figure 24).

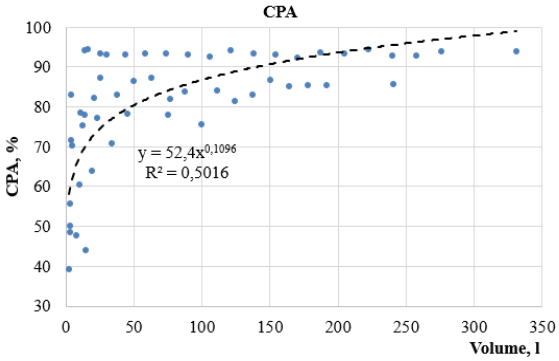

Fig. 23: The efficiency of the hydrate decomposition with an initial weight of 15 to 331 g

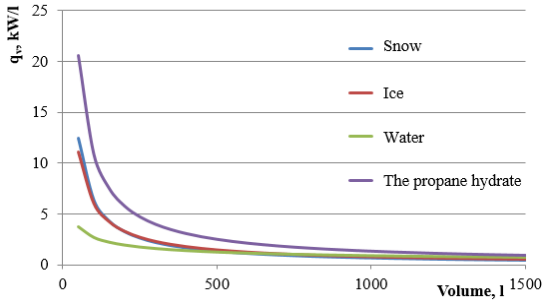

Fig. 24: Comparison of the average intensity of volumetric sources for snow, ice, water and hydrate

The combined graph in Figure 24 shows that the worst microwave radiation absorbs water. For a small amount of ice and snow (up to 0.5 liters), radiation absorption is better than that of water. Moreover, ice and snow in this respect behave in approximately the same, way apparently due to almost identical crystalline structure. When the volume of the substance begins to occupy a significant part of the chamber space (1-1.5 liters), there is a decrease in the intensity and alignment of heat sources for the liquid and solid phases of the water. The greatest absorption is characteristic of propane hydrate in the whole range of volumes. After approximating the average value of bulk sources in propane hydrate, we obtain a function

$$q_V = \frac{751,76}{V_g^{0,92}}. \quad (29)$$

Calculations show that for volumes more than 0.5 liters, electromagnetic radiation in the propane hydrate is 1.5 times better than in water and it is 1.74 times better than in ice and snow.
Analysis of the data indicates the commonality of microwave irradiation of various substances: water, ice, snow and hydrate. All of them are functions that are inversed in the volume of substance. However, the different structure of these substances leads to the emergence of bulk sources of heat of varying intensity. The intensity of sources in a small amount of water (up to 200 ml) is 2-3 times lower than their intensity for snow and ice of the same amount.
At larger volumes of water and ice, the intensity of volumetric heat sources becomes approximately the same. The curves of volumetric heat consumption for ice and snow, which have a similar structure, are also very similar.
The volumetric heat sources that occur inside the propane hydrate by the action of microwave radiation are 1.5 times greater than in water and 1.74 times larger than in ice and snow. For large quantities of material, the efficiency of the absorption of EM fields is 90% on average. The obtained results of field studies are the basis for comparison with the results of mathematical modeling.

3. Conclusions

In order to study the process of dissociation of hydrate under the influence of microwave electromagnetic radiation, series of field experiments were conducted, a mathematical model was developed and a series of studies were performed. The results of experimental studies of dissociation of gas hydrate allowed drawing the following conclusions.
1. It has been confirmed that the influence of the volumetric sources of heat, and not the influence of the boundary conditions, is the dominant influence on hydration dissociation under the action of microwave radiation. This provision formed the basis of the mathematical modeling of the dissociation of the hydrate massif.
2. It has been established that processes of heating water, melting ice and snow, and hydrate dissociation occur in a similar way. It is characteristic that the inverse proportional dependence of internal specific heat sources is obtained on the volume of material, that is the decrease in the efficiency of the radiator when the volume of the material is reduced.
3. It was established that the volume heat sources that occur inside the propane hydrate under the influence of microwave radiation are 1.5 times higher than in water and 1.74 times higher than in ice and snow. The absorption hydrate of the electromagnetic field at a frequency of 2.4 GHz is 90% for large quantities.

Acknowledgement

The work was carried out at Poltava National Technical Yuri Kondratyuk University, and its main results were realized within state-funded applied research work “Investigation of the influence of thermodynamic parameters of phase transitions in systems with gas hydrates on the efficiency of gas-hydrated technologies”, with the state registration number 0115U002420.

References

[1] Vedachalam, N., Srinivasalu, S., Rajendran, G., Ramadass, G. A., Atmanand, M. A. (2015). Review of unconventional hydrocarbon resources in major energy consuming countries and efforts in realizing natural gas hydrates as a future source of energy. *Journal of Natural Gas Science and Engineering*, 26, 163–175. doi: 10.1016/j.jngse.2015.06.008
[2] Makogon, Y. F., Holditch, S. A., Makogon, T. Y. (2007). Natural gas-hydrates – A potential energy source for the 21st Century. *Journal of Petroleum Science and Engineering*, 56 (1-3), 14–31. doi: 10.1016/j.petrol.2005.10.009
[3] Deusner, C., Bigalke, N., Kossel, E., Haeckel, M. (2012). Methane Production from Gas Hydrate Deposits through Injection of Supercritical CO_2. *Energies*, 5 (12), 2112–2140. doi: 10.3390/en5072112
[4] Oveckiy, S., Savchuk, V. (2016). A Method Developed to Increase Technological and Ecological Efficiency of Gas Production from Hydrate Deposits. *Eastern-European Journal of Enterprise Technologies*, 3, 10 (81), 41–47. https://doi.org/10.15587/1729-4061.2016.72545
[5] Chen, J., Wang, Y.-H., Lang, X.-M., Fan, S.-S. (2015). Energy-efficient methods for production methane from natural gas hydrates. Journal of Energy Chemistry, 24 (5), 552–558. doi: 10.1016/j.jechem.2015.08.014
[6] Pavlenko, A., Kutnyi, B., Holik, Yu. (2018). Study of the Effect of Thermobaric Conditions on the Process of Formation of Propane Hydrate. *Eastern-European Journal of Enterprise Technologies*, 5, 5 (89), 43–50. https://doi.org/10.15587/1729-4061.2017.111409
[7] Pavlenko, A., Kutnyi, B., Abdullah, N. (2017). A study of phase transition processes features in liquid-gas systems. *Eastern-*

European Journal of Enterprise Technologies, 4, 5 (88), 43–50. https://doi.org/10.15587/1729-4061.2017.108535

[8] Pavlenko, A., Kutnyi, B., Kugaevska, T. (2018) Research into resonance phenomena in gas-vapor bubbles, *Eastern-European Journal of Enterprise Technologies*, 1/5 (91), 39–47. https://doi.org/10.15587/1729-4061.2018.123957

[9] Kutnyi B.A. (2018) Termotechnical characteristics determination of enclosing structures for hydrates storage. *International Journal of Engineering & Technology*. 7, 510–515. https://doi.org/10.14419/ijet.v7i3.2.14580

[10] Leshchenko M. V., Semko V. O. Thermal characteristics of the external walling made of cold-formed steel studs and polystyrene concrete. *Magazine of Civil Engineering*. № 8, (2015), pp. 44–55. https://doi.org/10.5862/MCE.60.6

[11] Semko O., Yurin O., Avramenko Yu., Skliarenko S. Thermophysical aspects of cold roof spaces. *MATEC Web of Conferences*. Vol. 116, (2017), p. 02030. https://doi.org/10.1051/matecconf/201711602030

[12] Yurin O., Galinska T. Study of heat shielding qualities of brick wall angle with additional insulation located on the outside fences. *MATEC Web of Conferences*. Vol. 116, (2017), p. 02039. https://doi.org/10.1051/matecconf/201711602039

[13] Kutniy, B.A., Pavlenko, A.M. (2018) Mathematical modeling of the thermodynamic process gas-steam bubbles. *Academic journal Series: Industrial machine building, civil engineering*. Issue 1 (50). p. 220–226. ISSN 2409-9074

[14] Baba Babanli, M. Shumska, L., Leshchenko, M. (2018). Heat Treatment Technology of Porous Building Materials with Predictability of Thermophysical Properties. *International Journal of Engineering & Technology*, 7, № 3.2, 501–509. https://doi.org/10.14419/ijet.v7i3.2.1457

[15] Yurin, O., Azizova A. & Galinska, T. (2018). Study of heat shielding qualities of a brick wall corner with additional insulation on the brick Paper presented at the MATEC Web of Conferences, , 230 https://doi.org/10.1051/matecconf/201823002039